Chapter 2

Activity-Dependent Outgrowth of Neurons and Overshoot Phenomena in Developing Neural Networks

A. van Ooyen & J. van Pelt, J. Theor. Biol. 167 (1994) 27-43.

During the development of the nervous system, all kinds of structural elements such as neurons, neuritic extensions and synapses are initially overproduced (so-called overshoot phenomena).

Neurite outgrowth has been found to be regulated by electrical activity of the neuron. High levels of activity, resulting in high intracellular calcium concentrations, cause neurites to retract whereas low levels of activity, and consequently low calcium concentrations, allow further outgrowth. Using simulation models, we demonstrate that such activity-dependent outgrowth in combination with a neuronal response function with some form of firing threshold - which gives rise to a hysteresis effect - is sufficient to cause an overshoot with respect to connectivity or synapse numbers. As a consequence of hysteresis, the network connectivity at which a phase transition occurs from the quiescent to the activated state is higher than that for maintaining activity at a level where connectivity remains constant. A developing network will therefore first increase its connectivity until it becomes activated, upon which the neurites begin to retract. Connectivity then decreases until the equilibrium value is reached, thus causing the growth curve to exhibit overshoot.

2.1 Introduction

Neurons become assembled into functional neural networks during development. Among the many factors influencing the ultimate structure and function of the nervous system, electrical activity plays a pivotal role. Many mechanisms that determine neuronal connectivity such as neurite outgrowth, growth cone behaviour, naturally occurring cell death, trophic factors, synaptogenesis, elimination of synapses, and changes in synaptic strength have been found to be modulated by electrical activity (for review see Chapter 1 and Fields & Nelson, 1992).

Neurite outgrowth

Electrical activity of the neuron reversibly arrests neurite outgrowth (or produces retraction) and changes growth cone morphology (Cohan & Kater, 1986; Fields *et al.*, 1990a; Schilling *et al.*, 1991). Similarly, depolarizing media and neurotransmitters affect neurite outgrowth of many cell types (e.g., Sussdorf & Campenot, 1986; Lankdorf *et al.*, 1987; McCobb *et al.*, 1988; Lipton & Kater, 1989; Mattson & Kater, 1989; Todd, 1992), with excitatory neurotransmitters inhibiting outgrowth and inhibitory ones stimulating outgrowth.

Electrical activity and neurotransmitters probably regulate neurite outgrowth by affecting the calcium concentration in growth cones (Cohan *et al.*, 1987; Fields *et al.*, 1990b; Kater & Mills, 1991). This has led to the calcium theory of neurite outgrowth (e.g., Kater *et al.*, 1988; Kater *et al.*, 1990; Kater & Guthrie, 1990), which posits that low intracellular calcium concentrations ($[Ca^{2+}]_{in}$) stimulate outgrowth, higher concentrations cause a cessation of outgrowth, and still higher concentrations lead to regression of neurites. Thus, all factors that change $[Ca^{2+}]_{in}$ (such as action potentials or other forms of depolarization and neurotransmitter actions) are potentially able to affect neurite outgrowth. Alterations in $[Ca^{2+}]_{in}$ have also been implicated in the development of dendritic morphology (Kater *et al.*, 1990). Because of the morphological changes that accompany changes in $[Ca^{2+}]_{in}$, and the large number of signals that influence it, mechanisms regulating $[Ca^{2+}]_{in}$ have been proposed to represent a major means by which entire patterns of neuronal circuitry can be specified (Lipton & Kater, 1989).

Applied electric fields, too, influence nerve growth, with respect both to branching (McCaig, 1990a) and to the rate of elongation (McCaig, 1990b).

Network formation and overshoot

As a result of these activity-dependent processes, a mutual influence exists between the formation of synaptic connectivity and neuronal electrical activity. That is, a feedback loop exists between changes in network structure and changes in network activity (Von der Malsburg & Singer, 1988). This

feedback loop must be expected to have major implications for the stages a network goes through during its development.

A general feature of nervous system development, *in vivo* as well as *in vitro*, is that virtually all structural elements show an initial overproduction, followed by an elimination during further development. These so-called overshoot phenomena occur, for example, with respect to neuron numbers (e.g., Finlay & Slattery, 1983; Heuman & Leuba, 1983; Cowan *et al.*, 1984; for reviews see Oppenheim, 1991; Ferrer *et al.*, 1992), connections (e.g., Kato *et al.*, 1985; Stanfield & O'Leary, 1985; Price & Blakemore, 1985), total dendritic length (Uylings *et al.*, 1990), number of dendrites (Miller, 1988), number of axons (Schreyer & Jones, 1988; Gorgels *et al.*, 1989), number of synapses (e.g., Purves & Lichtman, 1980; Huttenlocher *et al.*, 1982; Warren & Bedi, 1984; O'Kusky, 1985; *in vitro*: Van Huizen *et al.* 1985, 1987a), receptors (e.g., Insel *et al.*, 1990; McDonald *et al.*, 1990; for review see McDonald & Johnston, 1990), and expression of neurotransmitters (e.g., Wahle & Meyer, 1987; Parnavelas *et al.*, 1988).

In most neural network models, the activity patterns of the system are studied in response to external input, given a particular collection of cells and network structure. In developing networks, however, the number of cells and network structure are variable and under control of the network activity itself (via the above mentioned activity-dependent processes). Furthermore, in the initial stages of development activity patterns that are not evoked by external input play a large role (also see Corner, 1990). Insight into the implications of activity-dependent processes and endogenous activity will therefore be indispensable for understanding the ontogenetic stages of the nervous system. In this article, we will address the implications of activity-dependent neurite outgrowth. It will be shown that this process can account for the occurrence of a transient overproduction of connections or synapse numbers.

No simulation models for explaining overshoot are known to us. In Feinberg *et al.* (1990) only a descriptive statistical model is presented for some overshoot phenomena *in vivo*.

2.2 The Model

The model is not meant to mimic a particular nervous system, but is rather used as a tool to gain insight into the role of activity-dependent outgrowth for network formation in general. We use a distributed model in which initially disconnected neurons organize themselves into a synaptically connected network by neurite outgrowth and synaptogenesis, under influence of endogenous activity (there is no external input). Growing neurons are modelled as expanding neuritic fields, and the outgrowth of each neuron depends upon its own level of electrical activity. Neurons become connected when their neuritic fields overlap. All connections are taken to be excitatory, considering that the predominant form of synaptic activity during early stages of devel-

opment appears to be excitatory (Jackson *et al.*, 1982; O'Brien & Fischbach, 1986; Habets *et al.*, 1987; Cherubini *et al.*, 1991; Corner & Ramakers, 1992). The model is inspired in part by tissue cultures of dissociated cerebral cortex cells (Van Huizen, 1986; Van Huizen *et al.*, 1985, 1987a; Ramakers *et al.*, 1991). As in the model, cells in such cultures become organized into a network without the influence of external or sensory input.

2.2.1 Neuron Model

The shunting model (Grossberg, 1988; Carpenter, 1989), which mirrors the underlying physiology of simple nerve cell dynamics (Hodgkin & Huxley, 1952), is used to describe neuronal activity. In this model, excitatory inputs drive the membrane potential towards a finite maximum (or saturation potential, e.g., the Na^+ equilibrium potential), while inhibitory inputs (if any) drive the membrane potential towards a finite minimum (e.g., the K^+ equilibrium potential).

For a purely excitatory network, the shunting model becomes

$$\frac{dX_i}{dt} = -\frac{X_i}{\tau} + (1 - X_i)\sum_{j=1}^{N} W_{ij}F(X_j), \tag{2.1}$$

where X_i is the (time averaged) membrane potential of neuron i, $F(X_j)$ is the firing rate of neuron j, W_{ij} is the coupling strength between neuron i and j ($W_{ij} \geq 0$; W_{ij} is defined in Section 2.2.2), and N is the total numbers of neurons. Thus, Eq. (2.1) takes the output of a neuron to be a mean firing rate. The effect of neuron j on X_i is mediated by trains of action potentials, and hence is proportional to the product of $F(X_j)$ and W_{ij}. The sum of all excitatory inputs, $\sum_{j=1}^{N} W_{ij}F(X_j)$, drives X_i towards the excitatory saturation potential, which is set equal to 1. In the absence of inputs, X_i decays, with a rate determined by $1/\tau$, to the resting potential, which is set equal to 0. Thus, X_i is scaled between 0 and 1. The initial values of X_i are set below the saturation potential (i.e., $X_i < 1$). The firing rate function F is a sigmoidal function of the membrane potential:

$$F(X) = \frac{1}{1 + e^{(\theta - X)/\alpha}}, \tag{2.2}$$

where $F(X)$ is the firing rate [with its maximum set to 1, see Fig. 2.7(a)], α determines the steepness of the function and θ represents the firing threshold. The low firing rate when X is sub-threshold may be considered as representing spontaneous activity, arising from threshold fluctuations (Verveen, 1960), membrane potential fluctuations, synaptic noise (Korn & Faber, 1987), and/or random external input. Equation (2.1) and similar ones have been widely used in the field of neural network modelling (Grossberg, 1988; and references therein)

2.2.2 Outgrowth and Connectivity

Neurons are randomly placed on a two-dimensional surface. In order to model outgrowth and formation of connections, each neuron is given a circular 'neuritic field', the radius of which is variable. When two such neuritic fields overlap, both neurons, say i and j, become connected to each other with a strength proportional to the area of overlap:

$$W_{ij} = A_{ij}c, \tag{2.3}$$

where $A_{ij} = A_{ji}$ is the amount of overlap ($A_{ii} = 0$) and c is a constant of proportionality; A_{ij} may be regarded as representing the total number of synapses formed between neuron i and j, while c could represent the synaptic strength. In this abstraction, no distinction has been made between axons and dendrites. If one were to do so, this would lead to a connectivity matrix $\mathbf{W}$ that needs no longer be symmetric. In most of the simulations we used Eq. (2.3). Just in order to test whether asymmetry would affect the results, we also used

$$W_{ij} = A_{ij}C_{ij}, \tag{2.4}$$

where A_{ij} is as before and C_{ij} is uniformly distributed with mean c, so $\mathbf{W}$ becomes asymmetric.

In the model, the outgrowth of each individual neuron depends upon its own level of electrical activity. Since the effect of activity on outgrowth is mediated by $[Ca^{2+}]_{in}$ (Cohan *et al.*, 1987; Fields *et al.*, 1990b; Kater & Mills, 1991), and one of the consequences of the firing of action potentials is the influx of calcium ions (e.g., Hockberger *et al.*, 1989), leading to elevated $[Ca^{2+}]_{in}$, we take the outgrowth to be dependent upon the firing rate:

$$\frac{dR_i}{dt} = \rho G(F(X_i)), \tag{2.5}$$

where R_i is the radius of the circular neuritic field of neuron i, and ρ determines the rate of outgrowth. The outgrowth function G is defined as

$$G(F(X_i)) = 1 - \frac{2}{1 + e^{(\epsilon - F(X_i))/\beta}}, \tag{2.6}$$

where ϵ is the value of $F(X_i)$ for which $G = 0$ and β determines the steepness of the function. The function G remains in the bounded range $< -1, 1 >$. Depending on the firing rate, a neuritic field will grow out ($G > 0$ when $F(X_i) < \epsilon$), retract ($G < 0$ when $F(X_i) > \epsilon$) or remain constant ($G = 0$ when $F(X_i) = \epsilon$) (see Fig. 2.1).

Equation (2.6) is simply a phenomenological description of the theory of Kater *et al.* (Kater *et al.*, 1988; Kater *et al.*, 1990; Kater & Guthrie, 1990) that the electrical activity of a neuron affects (via calcium influx) its outgrowth. High activity or $[Ca^{2+}]_{in}$ produces retraction, as reported in

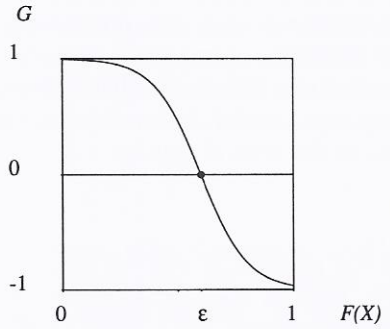

Fig. 2.1 Outgrowth function G [Eq. (2.6)].

Cohan & Kater (1986), Fields *et al.* (1990a) and Schilling *et al.* (1991), and low activity or $[Ca^{2+}]_{in}$ allows outgrowth. This description is also in agreement with observations that suppression of activity favours neurite outgrowth (Van Huizen & Romijn, 1987; Schilling *et al.*, 1991). An admittedly unrealistic property of Eq. (2.6) is that if $F(X_i) < \epsilon$, a neuron could grow out indefinitely. We preferred, however, not to put explicit bounds on the neuritic field size, because it appeared that the network itself is capable of regulating the size of its neurons.

Essential in the formulation of the outgrowth model is that connectivity can change during development. Using growing neuritic fields and taking the connection strength proportional to the area of overlap is just one way of achieving this. In addition, we have studied several other ways of changing connectivity (see Section 2.4).

To summarize, each neuron is described by differential equations for both the membrane potential X and the radius of the neuritic field R. In total, the model thus consists of $2N$ differential equations, where N is the total the number of neurons. The connectivity matrix $\mathbf{W}(N \times N)$ is variable and is determined by calculating the degree of overlap of the neuritic fields. The model is studied both analytically and by means of numerical solution, employing the variable time step Runge-Kutta integrator provided by Press *et al.* (1988).

2.2.3 Parameters

The membrane time constant τ was set at 8 ms, which is well within the range of values reported for cortical cells (Connors *et al.*, 1982) and hippocampal cells (Lacaille *et al.*, 1987). However, the results will appear not to depend upon the actual choice for τ. The outgrowth of neurons is on a time scale of days or weeks (Van Huizen *et al.*, 1985, 1987a; Van Huizen, 1986; Ramakers

et al., 1991; Schilling *et al.*, 1991), so that connectivity can be regarded as quasi-stationary on the time scale of membrane potential dynamics (i.e., ρ much smaller than $1/\tau$). To avoid unnecessarily slowing down the simulations, ρ was chosen as large as possible so as to maintain the quasi-stationary approximation. In most simulations, we used $\rho = 2.5 \cdot 10^{-6}$. As nominal values for the other parameters, we choose $\theta = 0.5$, $\alpha = 0.10$, $\beta = 0.10$ and $\epsilon = 0.60$. The effect of other values was studied in order to test the robustness of the results (Section 2.4).

2.3 Results

2.3.1 Global Model Behaviour

The behaviour of the model can in part be predicted directly from Eq. (2.1). The excitatory network defined by Eq. (2.1) ($W_{ij} \geq 0$; W_{ij} need not equal W_{ji}) has, for biologically realistic initial conditions ($X_i < 1$), convergent activation dynamics (Hirsch, 1989): every trajectory converges to some equilibrium point. The equilibrium states for a given $\mathbf{W}$ are given by the solutions of

$$0 = -\frac{X_i}{\tau} + (1 - X_i) \sum_{j=1}^{N} W_{ij} F(X_j) \qquad \forall i. \tag{2.7}$$

If the variations in X_i are small (i.e., relative to $\bar{X}$), we find for the average membrane potential of the network (see Appendix):

$$0 \simeq -\frac{\bar{X}}{\tau} + (1 - \bar{X}) \bar{W} F(\bar{X}), \tag{2.8}$$

where $\bar{W} = (1/N) \sum_{i=1,j=1}^{N} W_{ij}$. By means of numerical simulation, it was confirmed that Eq. (2.8) captures the essentials for qualitatively describing the global behaviour of the model in terms of $\bar{W}$ and $\bar{X}$ (see Section 2.3.2). Based on this approximation, $\bar{W}$ can be written as a function of $\bar{X}$:

$$\bar{W} = \frac{\bar{X}/\tau}{(1 - \bar{X}) F(\bar{X})} \qquad 0 \leq \bar{X} < 1, \tag{2.9}$$

which gives the steady state ($d\bar{X}/dt = 0$) dependence on $\bar{W}$ (Fig. 2.2). The steady states lying on the branch ABC (quiescent states: $\bar{X}$ is low) and on DEF (activated states: $\bar{X}$ is high) are stable, whereas those on CD are unstable. Thus for $W_1 < \bar{W} < W_2$ (W_1 and W_2 are the critical points), there exist two stable steady states (also see Murray, 1989). For slowly increasing $\bar{W}$ (starting at A) the path followed by $\bar{X}$ is different from that for slowly decreasing $\bar{W}$ (starting at F): $ABCEF$ and $FEDBA$, respectively. The presence of this hysteresis loop underlies the emergence of overshoot.

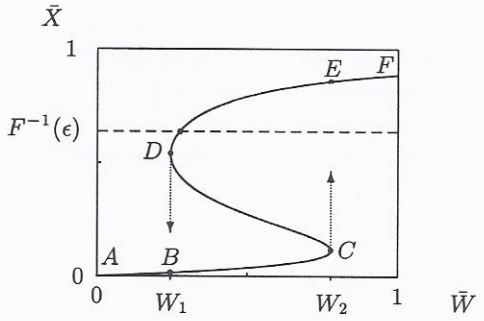

Fig. 2.2 Hysteresis. Steady state ($d\bar{X}/dt = 0$) dependence on $\bar{W}$ ($\bar{W} = (1/N)\sum_{i=1,j=1}^{N} W_{ij}$), according to Eq. (2.9). Further see Section 2.3.1 of text.

The size of the neuritic fields, and therefore $\bar{W}$, is governed by the system itself, being under control of neuronal activity. A neuritic field remains constant for $G = 0$, i.e., if $X_i = F^{-1}(\epsilon)$ [Eq. (2.6)], where F^{-1} is the inverse function of F. If this holds for all cells, $\bar{W}$ remains constant. Then, since all cells have identical ϵ, also $\bar{X} = F^{-1}(\epsilon)$. Thus, the equilibrium point of the system is the intersection point of the line $\bar{X} = F^{-1}(\epsilon)$ with the curve of Fig. 2.2. The rate of outgrowth is so low relative to the dynamics of the membrane potential that, for changing $\bar{W}$, $\bar{X}$ follows the curve. Starting with initially disconnected cells ($\bar{W} = 0$), the model can display four qualitatively different kinds of global behaviour (see Fig. 2.3), depending on the position of the equilibrium point (which is stable on the branches DE, EF and ABC, and unstable on CD).

DE: overshoot

Because the activity in the network is initially low, dR_i/dt is positive and $\bar{W}$ increases, whereby $\bar{X}$ follows the branch ABC until it reaches W_2, at which point $\bar{X}$ jumps to the upper branch, thus exhibiting a phase transition from quiescent to activated state. The activity in the network is then however so high [i.e., above $F^{-1}(\epsilon)$], that the neuritic fields begin to retract ($dR_i/dt < 0$) and $\bar{W}$ to decrease, whereby $\bar{X}$ moves along the upper branch from E to the intersection point. Thus, in order to arrive at an equilibrium point on the branch DE, a developing network has to go through a phase in which $\bar{W}$ is higher than in the final situation, thus exhibiting a transient overshoot in $\bar{W}$. number of synapses or connections in the network.

In Section 2.4, it will be shown that the existence of a hysteresis loop hinges upon the firing rate function F having a firing threshold and low but non-zero values for sub-threshold membrane potentials. The size of the

hysteresis loop depends on α (Fig. 2.7). A smaller α results in a larger hysteresis loop and a larger overshoot in $\bar{W}$. Since for small $\bar{X}$ the increase of $\bar{X}$, starting with $\bar{W} = 0$ and $\bar{X} = 0$, is proportional to $\bar{W}F(\bar{X})$ [see Eq. (2.1)], and the increase in $F(\bar{X})$ is relatively slow due to F being concave for $X < \theta$, $\bar{X}$ increases mainly as the result of increasing $\bar{W}$. Thus, the lower the value of $F(X)$ for sub-threshold values of X (i.e., α small), the higher $\bar{W}$ should become to activate the network (if $F(X) = 0$ for low X, one would need infinitely high $\bar{W}$), resulting in a larger hysteresis loop. Once $F(\bar{X})$ is high, $\bar{W}$ may be lower to keep $\bar{W}F(\bar{X})$ high. In other words, a higher $\bar{W}$ is needed to trigger activity in a quiescent network than to sustain it once the network has been activated.

ABC and EF: no overshoot

If the neuritic fields start retracting already at a very low level of activity, or only when the level of activity is very high, no overshoot occurs. In the first case, the equilibrium point lies on ABC, and the neurons stop growing even before $\bar{W}$ can reach the critical point W_2. In the second case, the equilibrium point lies on EF, and $\bar{W}$ will remain increasing after $\bar{X}$ has jumped to the upper branch, which is followed until the intersection point is reached.

CD: oscillations

An intersection point on this branch is unstable and results in regular oscillations that follow the path $ABCEDBCEDBC\ldots$. The period of these oscillations is determined by the value of ρ.

2.3.2 Simulation Results

Approximation

The validity of approximating the global behaviour of the network by Eq. (2.8) was confirmed by numerical simulation (Fig. 2.3). Generally, it was found that this approximation is good whenever the synaptic strength c is such that, at the time that (part of) the network approaches the transition to the activated state, the connectivity matrix $\mathbf{W}$ is a connected graph, i.e., there is a path from each cell to any other cell (see Peretto & Niez, 1986). This can be achieved if c is low, so that for the network to become activated each cell has to be connected to a number of neighbouring cells. If c is too high, on the other hand, the network breaks up into sub-networks [see Fig. 2.5(e)], in which the transition to the activated state may take place at different times, depending on the local cell density. The phase transition of the whole network is then fragmented and less clear-cut: in some parts of the network the cells may already be retracting, while in others they are still growing out. (In Fig. 2.3(a) the relative overshoot is larger than in Fig. 2.4 because c is smaller). The approximation is then no longer valid. Initially, Eq. (2.8) is

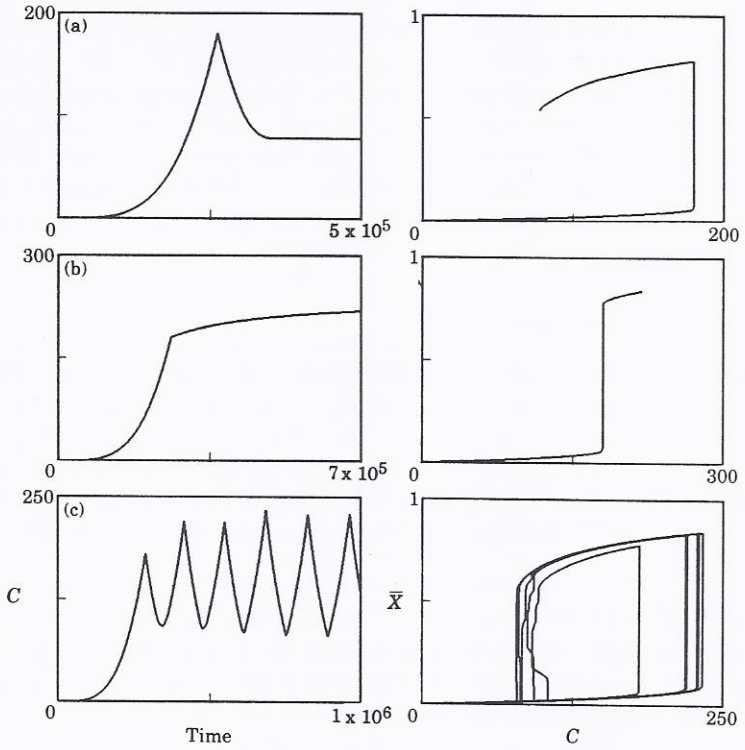

Fig. 2.3 Behaviour of the model (with $c = 0.1$, $N = 64$) for different values of ϵ. Connectivity C, against time, and against average membrane potential $\bar{X}$. $C = (1/2)\sum_{i=1,j=1}^{N} A_{ij}$ = total area of overlap = $(N\bar{W})/(2c)$. **(a)** Overshoot in connecticity, $\epsilon = 0.60$. **(b)** No overshoot, $\epsilon = 0.97$. **(c)** Oscillations, $\epsilon = 0.30$.

always a good approximation, because development starts with disconnected cells. At equilibrium, the network is exactly described by Eq. (2.8), since then $X_i = F^{-1}(\epsilon)$, $\forall i$.

Local behaviour

Except for their position, all the cells are exactly identical. Local variations in cell density, however, suffice to generate a great variability among individual cells, with respect both to their neuritic field size at equilibrium [Fig. 2.5(b), (d), (e), (f)] and to their developmental course of field size and firing behaviour (Fig. 2.4).

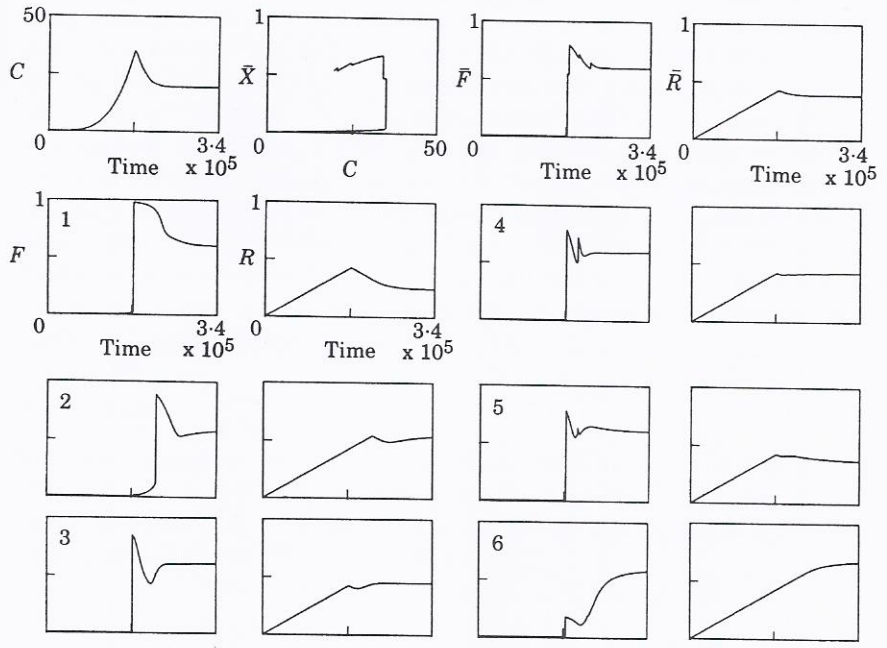

Fig. 2.4 Local behaviour. Same network as in Fig. 2.5. $C = (1/2)\sum_{i=1,j=1}^{N} A_{ij}$ = total area of overlap = $(N\bar{W})/(2c)$. In the first row the average behaviour of the network is shown; 1,...,6 are individual cells. Note that the relative overshoot in $\bar{R}$ is less than in C because (i) C is an area and R_i a radius; and (ii) R_i contributes to C only if the neuritic fields actually overlap.

All cells will attain a fixed equilibrium size for which the input from overlapping cells is such that $F(X_i) = \epsilon$, $\forall i$. Cells surrounded by a high number of neighbouring cells tend to become small since a small neuritic field will already give sufficient overlap with other cells. In contrast, relatively isolated cells must grow large neuritic fields in order to contact a sufficient number of cells. One might say that the neuritic fields adapt to the available space so as to cover it optimally. Because all cells have the same firing rate function and ϵ value, the area of overlap with other cells, $\sum_{j=1}^{N} W_{ij}$, will be the same for all cells. This area is given by [using Eqs (2.6) and (2.7)]

$$\sum_{j=1}^{N} W_{ij} = \frac{F^{-1}(\epsilon)/\tau}{\epsilon(1 - F^{-1}(\epsilon))}. \tag{2.10}$$

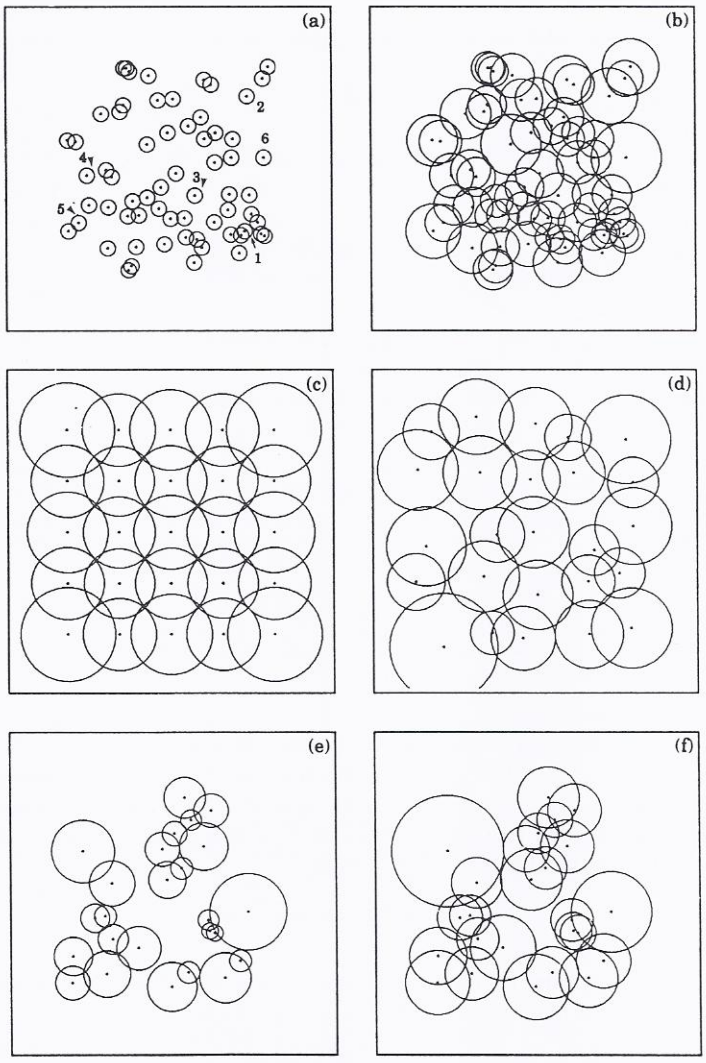

Fig. 2.5 Neuritic field sizes. **(a)** Early stage of development. The same network as in Fig. 2.3, but with $c = 0.4$ and $\epsilon = 0.6$. The numbers correspond to those in Fig. 2.4. **(b)** The same network as in (a) at equilibrium. Neuritic field size depends on local cell density. **(c)** Network ($N = 25$, $c = 0.2$) at equilibrium with cells at grid positions. **(d)** Network ($N = 25$, $c = 0.4$) at equilibrium with cells at noisy grid positions. **(e)** Network ($N = 25$) with high synaptic strength ($c = 2.5$), at equilibrium. Cells develop into sub-networks. **(f)** Same network as in (e) but with $c = 0.3$.

In dense parts of the network, the transition to the activated state takes place earlier than in less dense parts. Interaction between areas that are, and those that are not yet activated causes a range of developmental patterns in firing behaviour. A cell bordering on a cluster of cells with which it has contact at the moment the cluster makes a phase transition, will show a pattern like Fig. 2.4(3), in which the subsequent relatively rapid decrease in activity within this cluster, followed by further outgrowth of the border cell gives rise to a damped oscillation in firing rate. An isolated cell making contact with a cluster only after this cluster has gone through its phase transition (and to a large extent completed its subsequent decrease in field sizes and activity levels), will show a pattern like Fig. 2.4(6). Since the activity within such a cluster remains essentially constant, this cell will continue to grow out until its overlap is such that $F(X_i) = \epsilon$. In contrast, a cell at the heart of such a cluster will display a pattern like Fig. 2.4(1).

Network size

Synaptic strength determines the size of the resulting network(s) [Fig. 2.5(e), (f)]. When c is low, cells develop into one, connected network, whereas a high c can result in a development into separate networks, because contact with fewer cells is sufficient for $F(X_i) = \epsilon$.

Timing of overshoot

In networks with a high density of cells, overshoot takes place earlier than in low density networks (where neurons have to grow for a longer period of time in order to make sufficient contacts). Also the higher the synaptic strength c, the earlier the overshoot will occur.

If activity is totally blocked, on the other hand, cells keep growing out, and no reduction in connectivity can take place at all.

2.4 Robustness

The robustness of the results was tested under different parameter values and alternative formulations of the model.

Firing rate function

The smaller α in Eq. (2.2) is, the steeper F and the larger the hysteresis loop will be, resulting in a more pronounced overshoot (see Fig. 2.7 and Section 2.3.1).

Lowering θ, which translates F to the left, also increases the firing rate at low X. Thus, without simultaneously lowering α, this would result in a smaller hysteresis loop. In Fig. 2.6(h), a firing rate function is used with $\theta = 0.2$ and $\alpha = 0.05$. In fact, F in Eq. (2.1) may be replaced by any other

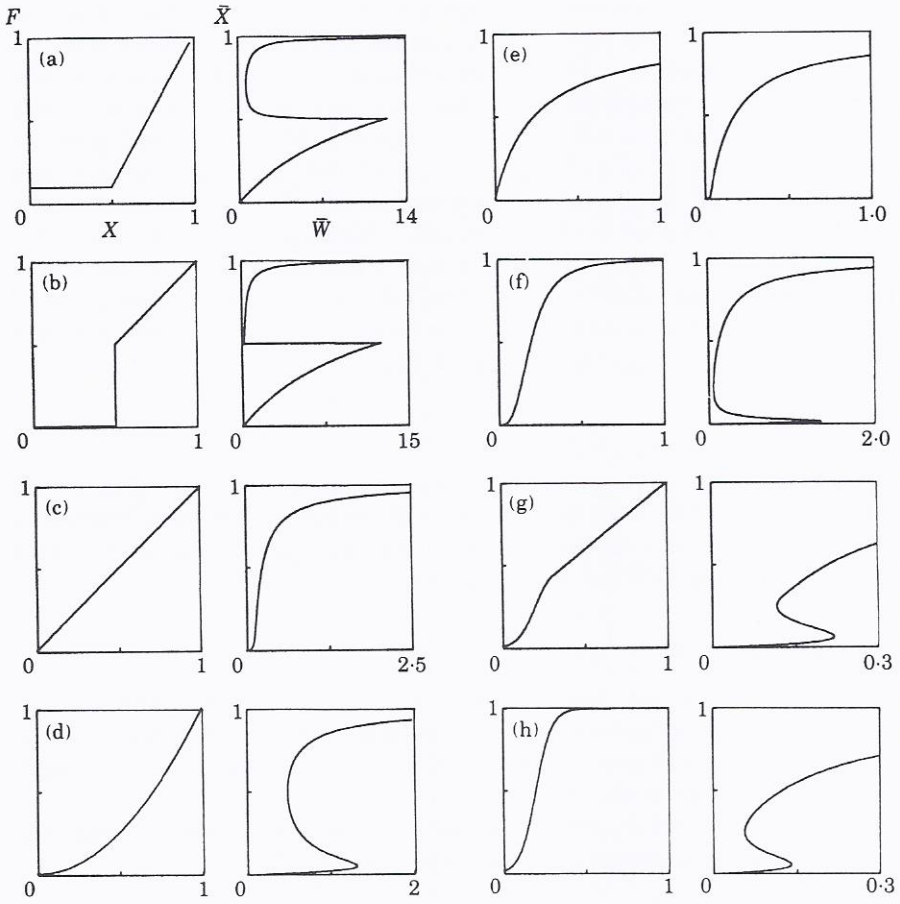

Fig. 2.6 Different firing rate functions (firing rate F versus membrane potential X) together with the curve defined by Eq. (2.9) ($\bar{X}$ versus $\bar{W}$). Except for linear and convex functions, all firing rate functions give rise to a hysteresis loop. **(a)** Piecewise linear. **(b)** Discrete threshold ($F = 0.01$ for $X < 0.5$). **(c)** $F = (1.0 - s)X + s$; $s = 0.01$. **(d)** $F = X^2 + s$; $s = 0.0025$. **(e)** $F = X/(X + K) + s$; $K = 0.25$, $s = 0.01$. **(f)** Sigmoidal function based on Michaelis-Menten function (De Boer & Perelson, 1991). $F = (1 - s)X^3/(\theta^3 + X^3) + s$; $\theta = 0.2$, $s = 0.001$. **(g)** Composite function. For $X \leq 0.3$, $F = 0.5/(1 + e^{(\theta - X)/\alpha})$ with $\alpha = 0.055$ and $\theta = 0.2$. For $X > 0.3$, F is linear. **(h)** Sigmoidal function according to Eq. (2.2), with $\alpha = 0.05$ and $\theta = 0.2$.

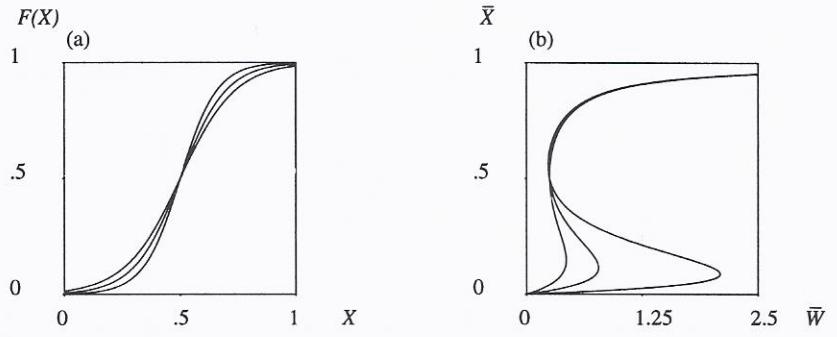

Fig. 2.7 The size of the hysteresis loop [Eq. (2.9)] depends on α of the firing rate function $F(X)$ [Eq. (2.2)]. **(a)** The smaller α, the steeper $F(X)$ and **(b)** the larger the hysteresis loop. Shown are $\alpha = 0.12$, 0.10 and 0.08.

function so long as the first part has a positive first and second derivative (or a discrete threshold) and $F(X) > 0$ for small X including $X = 0$. All these functions will give rise to hysteresis (Fig. 2.6).

Note that for overshoot to occur it is not essential that the firing rate during the phase transition jumps to a high value relative to its maximum, as it does with Eq. (2.2). Provided the value of ϵ is changed accordingly, a function like that of Fig. 2.6(g) can also be used.

Neuron model

As can be seen from Eq. (2.9), τ is only a scale factor and has no influence on the shape of the hysteresis curve. The general result is also obtained in some alternative formulations of the neuron model. For example, in the additive model (Grossberg, 1988):

$$\frac{dX_i}{dt} = -\frac{X_i}{\tau} + \sum_{j=1}^{N} W_{ij} F(X_j), \tag{2.11}$$

which lacks the factor $(1 - X_i)$ in Eq. (2.1), so X_i is no longer bounded. In analogy with Eq. (2.9) we obtain

$$\bar{W} = \frac{\bar{X}/\tau}{F(\bar{X})}, \tag{2.12}$$

which is plotted in Fig. 2.8(a) [with F according to Eq. (2.2)]. Because F is a sigmoidal, saturating function, $1 - X_i$ may be omitted without losing hysteresis. If, on the other hand, F is without bound (e.g., a power function) the saturating factor $1 - X_i$ is necessary for hysteresis.

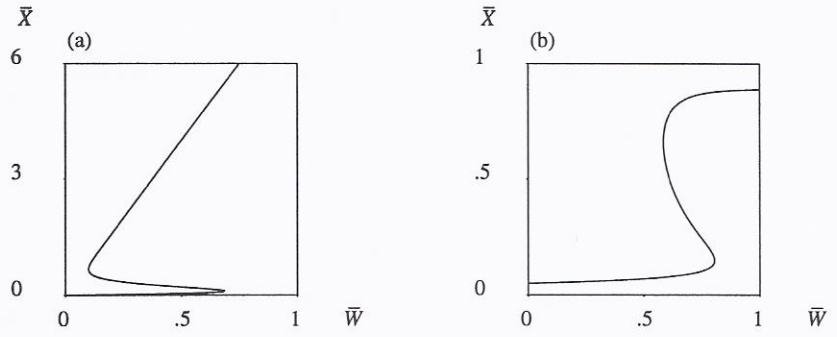

Fig. 2.8 Steady state dependence ($d\bar{X}/dt = 0$) on $\bar{W}$ for **(a)** additive model [Eq. (2.11)] and **(b)** model according to Eq. (2.13).

A modified form of Eq. (2.1) was introduced by Wilson & Cowan (1972):

$$\frac{dX_i}{dt} = -\frac{X_i}{\tau} + (1 - X_i)F(\sum_{j=1}^{N} W_{ij}X_j), \tag{2.13}$$

which replaces the sum of nonlinear signals in Eq. (2.1) by a nonlinear function of the sum. In analogy with Eq. (2.9) we obtain

$$F(\bar{W}\bar{X}) = \frac{\bar{X}/\tau}{1 - \bar{X}} \tag{2.14}$$

and, using Eq. (2.2)

$$\bar{W} = \left(\theta - \alpha ln(\tau/\bar{X} - \tau - 1)\right)/\bar{X} \qquad 0 < \bar{X} < \frac{\tau}{1+\tau}, \tag{2.15}$$

which is plotted in Fig. 2.8(b).

Network size

This is not a crucial parameter. The same phenomena are retained, for example, in a two-neuron model:

$$\begin{aligned} \frac{dX_1}{dt} &= -\frac{X_1}{\tau} + (1 - X_1)WF(X_2) \\ \frac{dX_2}{dt} &= -\frac{X_2}{\tau} + (1 - X_2)WF(X_1). \end{aligned} \tag{2.16}$$

The conditions for hysteresis and overshoot can now be formulated in terms of intersecting isoclines $dX_1/dt = dX_2/dt = 0$ (Fig. 2.9). In order for hysteresis

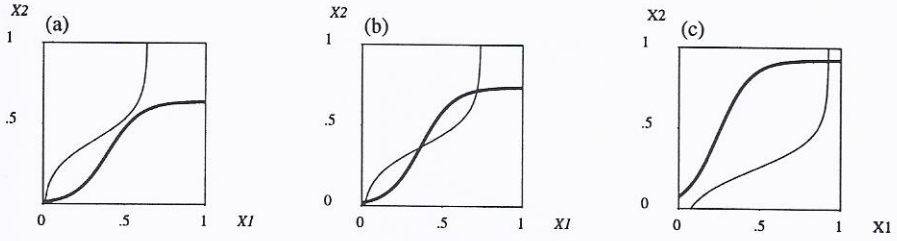

Fig. 2.9 Null-isoclines of the two-neuron model for **(a)** a low, **(b)** an intermediate and **(c)** a high value of W. The bold line is the X_2 isocline. For intermediate values of W, there exist three steady states, of which the middle one is unstable.

to occur there must be three equilibrium points (two stable and one unstable) for intermediate values of W. This can be achieved by sigmoidal isoclines (the form of the isoclines is determined by F and $1 - X_i$). Even a single neuron that is connected only to itself (Segal & Furshpan, 1990) is capable of displaying overshoot; the null-isocline is then exactly Eq. (2.8).

Outgrowth function

Parameter β in Eq. (2.6) determines the steepness of G. The form of the outgrowth function, however, affects only the specific time course of neurite outgrowth. In fact, any other function G for which $G > 0$ at low values of $F(X_i)$ and $G < 0$ at high values of $F(X_i)$ may be used. The same results are also obtained if outgrowth is made directly dependent on X_i, instead of on $F(X_i)$. The firing rate at which a neuritic field stabilizes, ϵ, is an especially important parameter of the model in that it determines whether or not overshoot will occur, and, if so, what its relative size will be.

Connectivity

Whether the connectivity matrix $\mathbf{W}$ is symmetric or asymmetric does not play a role in Eq. (2.9). This implies that modelling axons and dendrites separately would not affect the main findings. For example, using Eq. (2.4), with C_{ij} uniformly distributed between 0.0 and 0.8, yielded similar results as in the experiment of Fig. 2.4. The presence of hysteresis and overshoot also does not depend on the particular way in which connections between cells are defined. In Fig. 2.10 the results are shown of an experiment in which A_{ij} of Eq. (2.3) is simplified to $A_{ij} = 1$ if the neuritic fields of neuron i and j overlap, and $A_{ij} = 0$ if they do not. Even ignoring spatial structure by randomly filling in $\mathbf{W}$ gives the same general outcome.

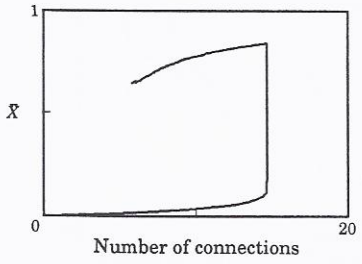

Fig. 2.10 The average membrane potential against the average number of connections. Number of connections $= (1/N)\sum_{i=1,j=1}^{N} A_{ij}$, in an experiment where A_{ij} of Eq. (2.3) is simplified to $A_{ij} = 1$ if neuron i and j overlap, and $A_{ij} = 0$ if they do not. With $N = 25$, $c = 0.05$, $\epsilon = 0.65$ and $\rho = 5.0 \cdot 10^{-5}$.

Variation

The results are robust with respect to differences in intrinsic properties, e.g., by randomly drawing cell parameters from uniform distributions. Thus, with α uniformly distributed over $[0.08, 0.12]$, $\tau \sim U[7, 10], \theta \sim U[0.4, 0.6], \epsilon \sim U[0.6, 0.8], \beta \sim U[0.08, 0.12]$, and $c = 0.1$ and $N = 64$, similar results were obtained as in Fig. 2.3. Thus, overshoot can also occur in networks composed of different cell types.

A network in which ϵ is distributed over a range of values that includes unstable ones, can still show overshoot as a whole, although the dynamics of the individual cells may be very complex (see Chapter 3).

External input

The neuron model with external input becomes

$$\frac{dX_i}{dt} = -\frac{X_i}{\tau} + (1 - X_i)\left\{E_i + \sum_{j=1}^{N} W_{ij}F(X_j)\right\} - (1 + X_i)I_i, \qquad (2.17)$$

where E_i and I_i are external excitatory and external inhibitory input, respectively; the inhibitory saturation potential is set to -1. In analogy with Eq. (2.9) we obtain

$$\bar{W} = \frac{\bar{X}/\tau - (1 - \bar{X})\bar{E} + (1 + \bar{X})\bar{I}}{(1 - \bar{X})F(\bar{X})} \qquad -1 < \bar{X} < 1, \qquad (2.18)$$

which is plotted in Fig. 2.11 for ($\bar{E} = 0.015$, $\bar{I} = 0$), ($\bar{E} = \bar{I} = 0$; normal situation), and ($\bar{I} = 0.008$, $\bar{E} = 0$). Without adjusting α, external excita-

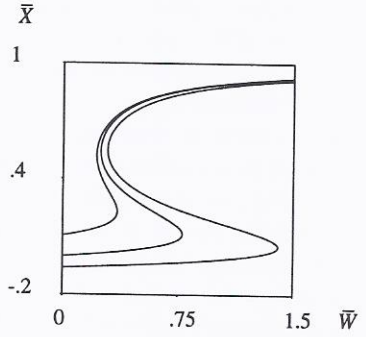

Fig. 2.11 Effect of external input. External excitatory input makes the hysteresis loop smaller, whereas inhibitory input makes it larger. Eq. 2.18 for $\bar{E} = 0.015$, $\bar{I} = 0$; $\bar{E} = \bar{I} = 0$ (normal situation), and $\bar{I} = 0.008$, $\bar{E} = 0$.

tory input makes the hysteresis loop smaller, while inhibitory input makes it larger. Thus, with excitatory input, α can be much lower - or even $F(X)$ such that $F(X) = 0$ for X below a certain value - and still not result in an excessively large hysteresis loop.

2.5 Comparison with Empirical Data

The results show some striking similarities, with respect to development of electrical activity, cell morphology, and connectivity, with what has been observed in developing *in vitro* cultures of dissociated cells.

The sequence of events in the model, with an initial phase of neurite outgrowth while electrical activity is low, an abrupt transition to high activity when connectivity reaches a critical value, and a phase with neurite retraction thereafter, has also been observed in cerebellar cultures (Schilling *et al.*, 1991). Purkinje cell dendrites elongate steadily during the first week after plating, when electrical activity is still negligible. As a result of cells becoming integrated into a functional neuronal network, electrical activity increases dramatically between 7-10 days *in vitro*. During this transition period dendrites cease their linear growth, retract, and then begin to branch profusely (in our model implementation, using neuritic fields, no separate branching events are distinguished). Coinciding with this period, there is an increase in $[Ca^{2+}]_{in}$. The notion that electrical activity, presumably by enhancing $[Ca^{2+}]_{in}$, might regulate dendritic growth patterns was further supported by the observation that blockade of electrical activity resulted in the continued elongation of dendrites as well as a decrease in $[Ca^{2+}]_{in}$. The developmental sequence described above applied to all Purkinje cells, but the actual tim-

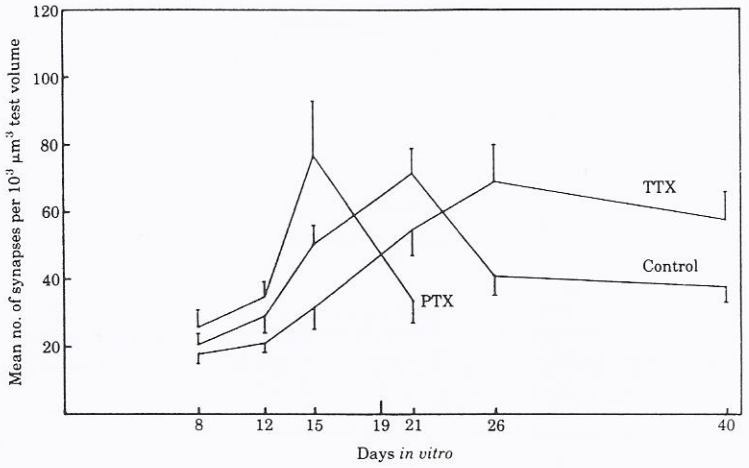

Fig. 2.12 Cultures of dissociated cerebral cortex cells show a transient overproduction of synapse numbers (control). Chronic blockade of activity (by TTX) largely prevents synapse elimination, whereas intensification (PTX) accelerates the process. After Van Huizen (1986).

ing varied for individual cells. Variations in timing are also observed in the model, and occur simply as a result of differences in local cell density. The model cells are capable at any time of changing the length of their neurites in response to changes in activity. Morphological changes in Purkinje cells, too, were found to be reversible, with even mature-looking cells altering their dendritic growth in response to changes in activity. Schilling *et al.* (1991) propose that in the absence of synaptic input dendrites will continue to elongate until they encounter active presynaptic elements. This view is consistent with our model, in which a disconnected cell will grow out until it has established sufficient contacts with active cells (see Section 2.2.2). It is also consistent with the synaptotrophic hypothesis of dendritic growth (Vaughn, 1989), which posits that growth and branching are initiated and maintained by synapses formed on growth cones.

As in the simulation model, cultures of dissociated cerebral cortex cells show a transient overproduction (overshoot) of synapses during development (Van Huizen *et al.*, 1985, 1987a; Van Huizen, 1986), with a phase of neurite outgrowth and synapse formation during the first three weeks *in vitro* being followed by a substantial elimination of synapses during the week thereafter (Fig. 2.12). The development of electrical activity in these cultures shows a good correspondence with what has been described above for cultured Purk-

inje cells (and for the simulation model). With increasing synaptic density, single neuron firing and network activity - which takes the form of repetitive slow field potentials (Corner & Crain, 1972; Van Ooyen *et al.*, 1992a, b) - abruptly appear within a window of a few days (Habets *et al.*, 1987). In such cultures, electrical activity appears to control both neurite outgrowth and synapse elimination: chronic blockade of electrical activity enhanced neurite outgrowth (Van Huizen & Romijn, 1987) and prevented synapse elimination during the fourth week (Van Huizen *et al.*, 1985). In contrast, chronic intensification of activity accelerated the formation of synapses and hastened the process of synapse elimination by almost a week (Van Huizen *et al.*, 1987a)(Fig. 2.12). The model responds in a similar way to suppression or intensification of electrical activity (see Section 2.3.2, *Timing of overshoot*).

Different cell types in the rat cerebral cortex show different growth curves with respect to radial distance and total dendritic length (Uylings *et al.*, 1990), with cells displaying clear, minor or no overshoot at all. Some of these curves show a clear resemblance to the ones observed in the model.

2.6 Conclusions and Discussion

Many of the processes that play a role in network development are dependent upon the electrical activity of the neurons and network itself, so that a tight coupling exists between network formation and network activity. In this study, we have examined the consequences for network ontogeny of one of these processes, namely activity-dependent neurite outgrowth. We have demonstrated that the very presence of this mechanism in combination with another elementary neuronal property - a non-linear neuron response function, i.e., a threshold for action potential generation - is sufficient to generate overshoot phenomena with respect to connectivity. The results are robust under: different firing rate functions (provided they have a type of firing threshold and low but non-zero values for sub-threshold membrane potentials, i.e., spontaneous activity); variance among neurons in all parameters; different neurite outgrowth functions (provided a high level of electrical activity results in retraction and a low level in outgrowth); symmetric versus asymmetric connectivity matrix; the way in which connections are defined; network size and different neuron models.

The mechanism underlying the generation of overshoot in this simple model may provide part of the explanation for overshoot phenomena in the developing nervous system, at least for those which have been observed in tissue cultures of dissociated cells. In such cultures, the sequence of events corresponds closely to that observed in the simulation model.

It should be emphasized that other, more realistic, descriptions of neurite outgrowth and synaptogenesis (e.g., with individual neurites instead of a circular neuritic field, and possibly some form of conservation of, or limit upon, the total numbers of synapses per cell rather than simply assuming

that the larger the overlap of neuritic fields, the more synapses will be made) are merely different mappings onto the connectivity matrix $\mathbf{W}$. Although this could affect the particular network structure, overshoot would still take place.

The neuritic field size of the model cells adapts to the local cell density, resulting in small fields in dense areas and larger ones in sparse areas. In this respect, it is interesting that the dendritic fields of ganglion cells, the cell bodies of which are arrayed in a regular mosaic, have been reported to achieve a uniform coverage of the retina so that every point of the visual space is 'seen' by at least one cell (Wässle *et al.*, 1981). From these observations it was inferred that some kind of growth mechanism must exist whereby local interactions among cells regulate dendritic field size. Activity-dependent outgrowth may be a candidate for such a mechanism.

Hysteresis may provide a mechanism by which overshoot phenomena in general can be understood. To illustrate this, consider the following variant of the model. Suppose that cell death is more likely at (very) high levels of electrical activity, and that neurons (whose neuritic fields are now taken to be constant) are produced at a given source, transported and incorporated into a network during development. As before, neurons become connected when their neuritic fields overlap. At a given cell density, the network will become activated and start losing cells if the resulting activity is too high. Because of hysteresis, a higher cell density is necessary to trigger activity in a quiescent network than to sustain it once the network has been activated, thus giving rise to a reduction in cell numbers. Such a transient overproduction of cells has been observed in the development of, for example, the suprachiasmatic nucleus (Swaab *et al.*, 1990). Another variant of the model would be one in which the neuritic fields are more or less constant and (partly) overlapping, while it is now the formation of new synapses or the strengthening of older ones which is activity-dependent. This would lead to exactly the same results, with overshoot in number of synapses or synaptic strength, respectively.

For some values of ϵ, the firing rate at which a given neuritic field remains constant, the model can generate sustained oscillations in overall activity (and connectivity). The period of these oscillations is determined by ρ, the rate of outgrowth of neuritic fields or, in the alternative formulations of the model, the rate at which synapses are formed/destroyed or existing ones are strengthened/weakened. Since these changes can occur on a time scale of hours, this mechanism might provide a possible explanation for the occurrence of slow rhythmic activity in various brain areas (e.g., circadian rhythms in the suprachiasmatic nucleus).

With respect to overshoot in connectivity, there may exist a parallel with the developing immune system. In the immune system, which may function as a network (Jerne, 1974), a high idiotypic connectivity (the number of clones with which a given clone interacts) is found during early ontogeny (Holmberg *et al.*, 1986). A possible explanation might be that highly connected clones, which become over-stimulated or suppressed if clones are large, can only

be maintained during early life when all clones are small and the network has not yet filled with antibodies (De Boer & Perelson, 1991). In analogy, neurons in our network can only maintain a high number of connections during early development when the network is not yet 'filled' with activity. Once the network is activated, these neurons become over-stimulated and subsequently lose some of their connections.

Overshoot phenomena may also be involved in learning. Doyle *et al.* (1992) presented evidence to suggest that information storage during learning may be based on connectivity changes mediated by a replay of early developmental events. In this concept, information acquisition may induce a transient overproduction of synaptic contacts in a given network, followed by an activity-dependent selection to yield a new circuitry.

The present study might also have relevance for understanding the ontogenetic origins of epilepsy. If, for whatever reason, activity is blocked during development, insufficient reduction in connectivity will result. This could lead in adulthood, assuming that pruning of connections is largely restricted to a 'critical period', to a network prone to epileptic-like activity because of its abnormally high degree of connectivity. Interestingly, Ben-Ari & Represa (1990) have suggested that use-dependent sprouting may play a role in epilepsy.

Damaging a proportion of the model cells results in increased neurite outgrowth of the remaining cells until all the cells have the same activity level as before. This is reminiscent of what happens following early prefrontal cortex lesions in rats. In such animals, an increase in dendritic arborization is found - possibly accompanied by synapse formation - which seems to correlate with the occurrence of behavioural sparing of function (Kolb & Kibb, 1991).

If the level of spontaneous activity is too low (or the synapses too weak) for the network to become activated by its intrinsic activity, neurites would continue growing out until at some stage during development the network may become activated by external input (e.g., sensory input). This could then result in retraction of neurites, the network being hyperactive due to its high degree of connectivity. Such a scenario would also give rise to overshoot. Age-related decreases in spine density and in total length of dendrites have indeed been reported for the development of Purkinje cells *in vivo* (Pentney, 1986). It may be hypothesized that changes in levels of electrical activity play a role in these morphological alterations.

The intracellular calcium concentration ($[Ca^{2+}]_{in}$) is likely to be one of the primary variables controlling neurite outgrowth. One of the factors that can change $[Ca^{2+}]_{in}$, and hence neurite outgrowth, is electrical activity, which, in turn, is dependent upon network connectivity and network dynamics. Therefore, the mechanisms regulating $[Ca^{2+}]_{in}$ may be major determinants of entire patterns of neuronal circuitry, as was suggested by Kater *et al.* (1988). Indeed, with the help of a relatively simple model of a developing neural network we have shown that activity-dependent neurite outgrowth can have a profound effect on network structure during development in that it generates pronounced overshoot phenomena with respect to connectivity.

Appendix

Derivation of Eq. (2.8). Taking the average over i in Eq. (2.7) and writing $X_i = \bar{X} + \Delta X_i$, with $\bar{X} = \frac{1}{N}\sum_{i=1}^{N} X_i$, yield

$$0 = -\frac{\bar{X}}{\tau} + \frac{1-\bar{X}}{N}\sum_{j=1}^{N} F(X_j)\sum_{i=1}^{N} W_{ij} - \frac{1}{N}\sum_{j=1}^{N} F(X_j)\sum_{i=1}^{N}\Delta X_i W_{ij} \qquad \text{(A.1)}$$

Take $\sum_{i=1}^{N} W_{ij} = N\bar{W}_{\cdot j}$, and write $W_{ij} = \bar{W}_{\cdot j} + \Delta_i W_{ij}$

$$0 = -\frac{\bar{X}}{\tau} + (1-\bar{X})\sum_{j=1}^{N} F(X_j)\bar{W}_{\cdot j} - \frac{1}{N}\sum_{j=1}^{N} F(X_j)\sum_{i=1}^{N}\Delta X_i \Delta_i W_{ij} \qquad \text{(A.2)}$$

If ΔX_i and $\Delta_i W_{ij}$ are uncorrelated or small:

$$0 \simeq -\frac{\bar{X}}{\tau} + (1-\bar{X})\sum_{j=1}^{N} F(X_j)\bar{W}_{\cdot j} \qquad \text{(A.3)}$$

Take $F(X_j) = F(\bar{X}) + \Delta X_j F'(\bar{X}) + ...$, and write $\bar{\bar{W}} = \frac{1}{N}\sum_{j=1}^{N}\bar{W}_{\cdot j}$, with $\bar{W}_{\cdot j} = \bar{\bar{W}} + \Delta\bar{W}_{\cdot j}$

$$0 \simeq -\frac{\bar{X}}{\tau} + (1-\bar{X})F(\bar{X})\bar{W} + (1-\bar{X})F'(\bar{X})\sum_{j=1}^{N}\Delta X_j \Delta\bar{W}_{\cdot j} + ..., \qquad \text{(A.4)}$$

where $\bar{W} = \sum_{j=1}^{N}\bar{W}_{\cdot j} = (1/N)\sum_{i=1,j=1}^{N} W_{ij}$.
If, again, ΔX_j and $\Delta\bar{W}_{\cdot j}$ are uncorrelated or small, and ignoring higher order terms in the Taylor expansion:

$$0 \simeq -\frac{\bar{X}}{\tau} + (1-\bar{X})\bar{W}F(\bar{X}).$$